Morphology of Southern Hemisphere Riometer Auroral Absorption

A.J. Foppiano
Departamento de Geofísica
Universidad de Concepción, Concepción
CHILE

foppiano@udec.cl

ABSTRACT

A morphology of riometer auroral absorption is derived from hourly values, determined at several Southern Hemisphere stations, located both near the centre of the auroral absorption zone and at higher and lower latitude fringes of the zone. Since spatial coverage of the data precludes a detailed morphology determination, use was made as guideline at all stages of an auroral absorption model derived for the Northern Hemisphere (NH). The day-to-day variability was first determined from cumulative amplitude-probability distributions calculated for a given hour at a given location for a range of geophysical conditions. These distributions are found to be well represented by log-normal distributions for most locations, times-of-day and solar and geomagnetic activity levels, over the range of absorption for which values are more accurate (typically 0.3 dB or above). Furthermore, parameters of log-normal distributions are found to be related following a known simple expression, so as to permit full specification of any distribution by a single parameter. Both these results are found to be consistent with the NH counterparts. Then time-of-day dependencies were determined for several distribution parameters. These were also found to show the same features than in the NH except for locations near the so-called South Atlantic Anomaly of the geomagnetic field. Determination of latitude and longitude dependencies are only possible when due account is taken of the widening and equator ward movement of the auroral absorption zone with increasing geomagnetic activity level. Assuming Gaussian latitude dependencies apply for all hours, longitude factors are determined so as to be consistent with observed geomagnetic activity level dependencies of absorption distribution parameters for the different longitudes. These factors lead to longitude dependence, which is consistent with theoretical and empirical evidence from other phenomena. This result seems to be different from that that holds for the NH.

1. INTRODUCTION

Knowledge of the morphology of ionospheric auroral absorption, experienced by high-frequency radio waves propagating at high latitudes, is of particular value for assessing radio communications performance. This can be derived from riometer measurements and applied to field strength prediction procedures [e.g. 1-5]. Although auroral absorption may also be determined from oblique-path field-strength observations [6], results from this method strictly apply only for locations where signals traverse the absorbing region, which are usually somewhat limited. Moreover, they may include uncertainties relating to the variability of path-mode parameters. On the other hand, riometer auroral absorption values have to be converted to oblique-path absorption prior to use in field strength prediction procedures, a process, which includes several assumptions. However, there are riometer measurements in the Northern Hemisphere (NH) for a wide range of locations and geophysical conditions, thus giving some advantage to their use to determine the morphology of auroral absorption.

Foppiano, A.J. (2006) Morphology of Southern Hemisphere Riometer Auroral Absorption. In *Characterising the Ionosphere* (pp. 4-1 – 4-26). Meeting Proceedings RTO-MP-IST-056, Paper 4. Neuilly-sur-Seine, France: RTO. Available from: http://www.rto.nato.int/abstracts.asp.

The purpose of this paper is to derive a morphology of riometer auroral absorption for the Southern Hemisphere (SH), which may lead to the development of an auroral absorption model similar to the one proposed many years ago for the NH [4]. This old model has been found more recently of some practical use [7,8] and as the base for new developments [9]. An extensive Southern Hemisphere data set of hourly values of riometer absorption is used. These are for several stations located at various longitudes near the centre of the southern auroral absorption zone and also at higher and lower latitudes. However, the spatial coverage of the data for the SH is far less than the used for the development of the NH model. This precludes a detailed morphology determination. As an alternative, the model derived for the NH is used as a guideline at all stages of the SH morphology determination. In the following section a very brief summary of the NH hemisphere is given. Section 3 describes the SH absorption hourly values data set used. The day-to-day variability of these values for different locations and geophysical conditions are discussed in Section 4 with reference to the known properties of this variability for the NH. Then, time-of-day, latitude and longitude dependencies are considered in Sections 5 to 7, together with the effect on these by the geomagnetic activity level.

2. BRIEF SUMMARY OF NH MODEL

The model gives the percentage of time, Q_A, a given riometer absorption, A dB, for a frequency of 30 MHz, is exceeded. This is calculated assuming that the cumulative amplitude probability of absorption values is given by a log-normal distribution, which can be specified by two parameters: Q_1, the percentage of time an absorption of 1dB is exceed and A_m, the median absorption, where A_m is proportional to Q_1. Q_1 is calculated using empirical formulae for a given location specified in terms of corrected geomagnetic latitude, corrected geomagnetic longitude, corrected geomagnetic local time, season (solar declination), and solar (R) or geomagnetic activity level (Kp or Ap). The formulae are given in the Annex. Figure 1 shows sample latitudinal dependencies of Q_1 for a given longitude, three local times, equinox and several geomagnetic activity levels. As can be clearly seen, the latitude dependence follows approximately a Gaussian function. Both the maximum absorption and the width of the distribution increase with increasing geomagnetic activity level. By contrast, the latitude of maximum absorption decreases with increasing level of geomagnetic activity. Sample time-of-day dependencies of Q_1 are shown in Figure 2 for a given location during equinox. In this case, both the morning and night absorption maxima increase with increasing geomagnetic activity level and the times at which these maxima occur also change with geomagnetic activity: the morning maximum occurring earlier as geomagnetic activity increases and the night maximum occurring earlier as latitude increases. The same longitude dependence applies for all latitudes, times-of-day and seasons. Figure 3 shows this longitude dependence as a factor multiplying all other dependencies. Absorption is larger for the Russian and Alaskan longitude sectors and less for the Canadian and Scandinavian sectors.

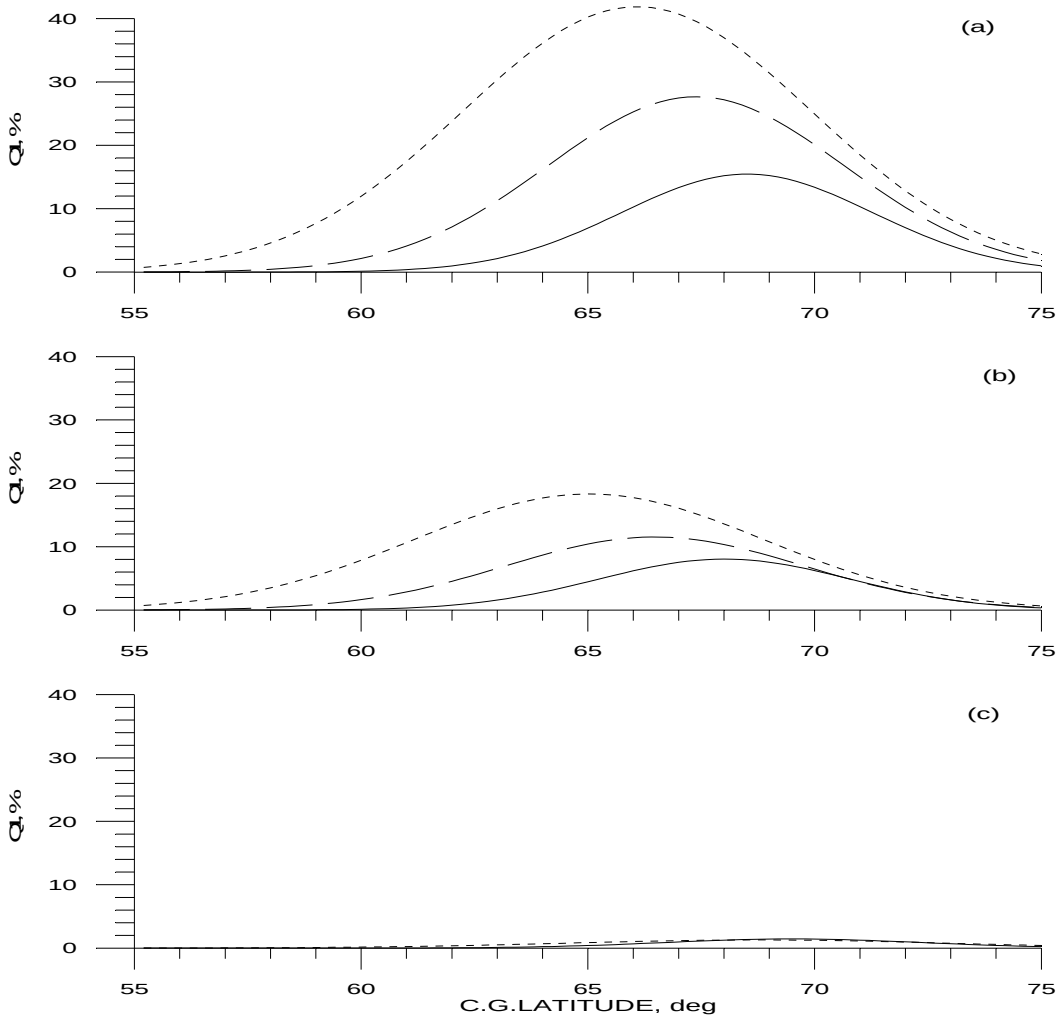

Figure 1. Latitudinal dependence of model Q1, percentage of time absorption at 30 MHz exceeds that of 1 dB, corresponding to different levels of geomagnetic activity (Ap=4, solid line; 9, dashed and 23, dotted). Values for Equinox (solar declination 0 degrees) and at the longitude of maximum Q1 (longitude 180 degrees). (a) morning maximum (10 h), (b) night secondary maximum (00 h) and (c) evening minimum (18 h). Corrected geomagnetic latitude, longitude and local time are used.

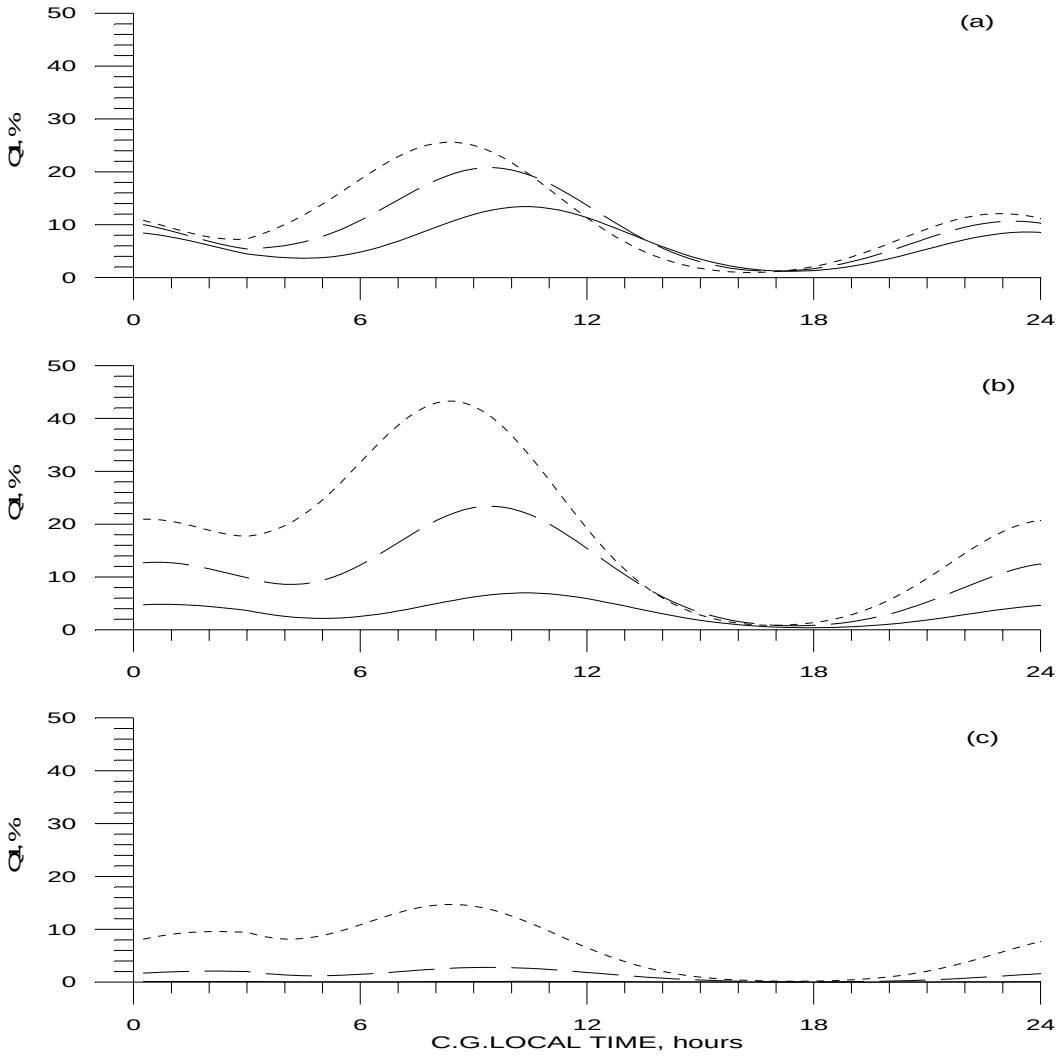

Figure 2. Time-of-day dependence of model Q_1, percentage of time absorption at 30 MHz exceeds that of 1 dB, corresponding to different levels of geomagnetic activity (Ap=4, solid line; 10, dashed and 27, dotted). Values for Equinox (solar declination 0 degrees) and at the longitude of maximum Q_1 (longitude 180 degrees). (a) northern fringe of absorption zone (70 degrees), (b) middle (65 degrees) and (c) southern fringe (60 degrees). Corrected geomagnetic latitude, longitude and local time are used.

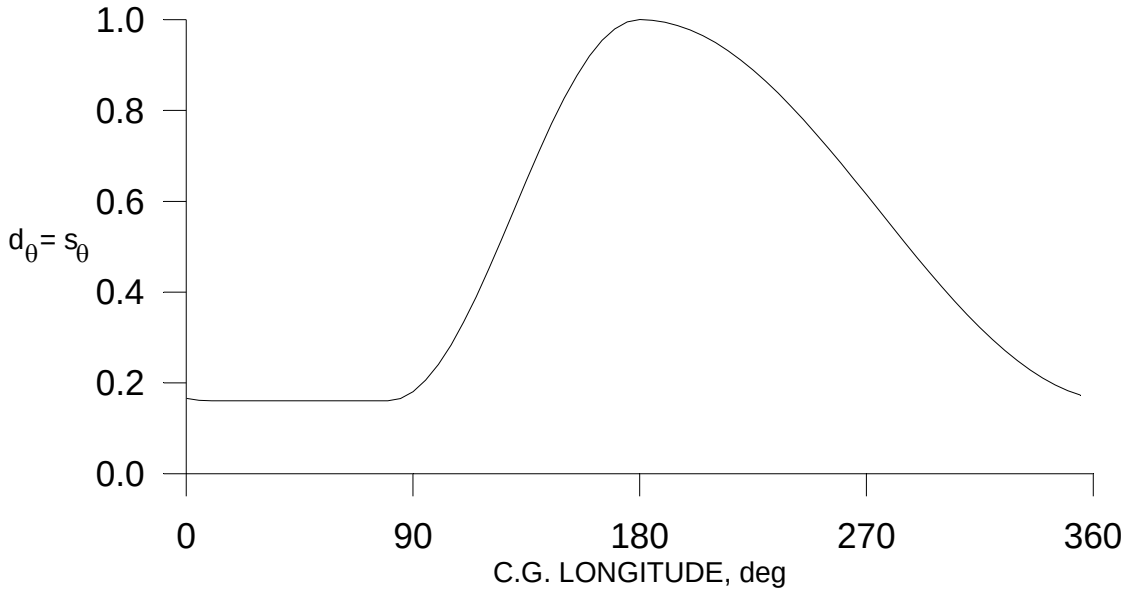

Figure 3. Longitude dependence of Q_1, percentage of time absorption at 30MHz exceeds that of 1 dB.

3. ABSORPTION HOURLY VALUES DATA SET

The analysis is performed with riometer absorption values which can be regarded as representative of conditions during the first minute of each hour (in some cases also the thirty-first minute value is used), of each day for the stations and time periods indicated in Table 1. The limited spatial coverage can be assessed from in Figure 4. In most cases the absorption has been computed with reference to monthly quiet day curves derived using the inflection point method described by Krishnaswamy et al. [10]. Absorption values for Syowa relate to monthly quiet day curves produced from sidereal-time diurnal variations of cosmic noise intensities, corresponding to several geomagnetic quiet days of the month [e.g.11]. Values for Novolazarevskaya are absorption in dB below a certain threshold given in units of noise power (H. Gernandt, private communication). It is difficult to compare the accuracy yielded by these different methods. However, most results can be regarded as precise to approximately 0.1 dB.

Table 1. Stations and time intervals for which hourly values of riometer absorption are used.

Station	Geographic Lat. deg.S.	Geographic Long. deg.	Corrected Geomagnetic Lat. deg.S.	Corrected Geomagnetic Long. deg.E.	Period	Riometer Frequency Mhz
Kerguelen	49.4	70.3E	58.4	121.4	1974-86	30.0
Halley Bay	75.5	26.6W	61.0	28.3	1974-78	27.6
Novolazarevskaya	70.8	11.8E	62.4	51.5	1980-82	23.0
					1983-86	32.0
Syowa	69.0	39.6E	66.1	70.9	1974-86	30.0
South Pole	90.0	-	74.0	19.5	1982-86	30.0
Terre Adelie	66.7	140.0E	80.7	235.4	1982-86	30.0

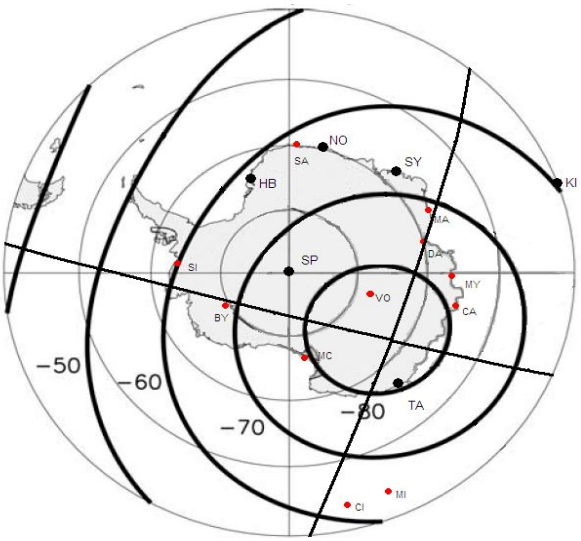

Figure 4. (large dots) Stations for which hourly values of riometer absorption are used. (thick lines) Approximate grid of corrected geomagnetic coordinates (adapted from Figure 1, [23]). (thin lines) Grid of geographic coordinates.

Although all riometer measurements were made using wide beam antennas, some differences may arise from the actual experimental settings. Also, the operating frequencies vary from station to station. Corrections for antenna beam-width are hardly feasible, both because in practice antenna performance often departs from theory and because theoretical calculations are quite unrealistic due to the patchy structure of the absorbing region across the solid angle subtended by the antenna [12]. Thus, only normalization to a standard frequency of 30 MHz has been made assuming that over the range of frequencies used an inverse-square frequency dependence approximately holds.

4. DAY-TO-DAY VARIABILITY

In particular, data are combined to test the applicability of the log-normal model for the observed cumulative amplitude-probability distributions, which has been already shown of some value [3,13,14]. Although Krishnaswamy [15] has analyzed a small part of this database, results from a more detailed statistical grouping are considered here. The method of analysis follows that of Foppiano and Bradley [16].

4.1. Amplitude-probability distributions

As expected from previous studies of riometer absorption morphology, one must consider variations with time of day, latitude, longitude, season and levels of solar and geomagnetic activity. However, grouping data to take into account these variations significantly reduces sample sizes, leading to unstable amplitude-probability distributions. Here a sample size of around 300 is considered appropriate. Hargreaves et al. [17] discusses sample size effects in more detail.

Over two thousand cumulative amplitude-probability distributions of riometer absorption have been determined by noting, for each station and each hour, the number of days with absorption in the following bands: 0-1 dB in 0.1 dB steps; 1-2 dB in 0.2 dB steps; 2-5 dB in 0.5 dB steps; and in 1 dB steps from 5-10 dB. Larger absorption values were ignored, on the assumption that they are mostly associated with polar cap absorption events. Periods of one year at a time have been used for all stations to investigate the effects of solar activity level. Intervals relating to various levels of geomagnetic activity as measured by the monthly mean Ap index, selected from all years are used for corresponding effects, as indicated in Table 2. As can be observed, sample sizes to determine seasonal variations are rather small.

Table 2. Geomagnetic activity levels used to group hourly values of riometer absorption

Station	Monthly mean Ap	Total months	Number of months according to season			
			Spring	Summer	Autumn	Winter
Halley Bay	8-10	11	3	5	0	3
	11-12	9	3	1	2	3
	13-14	9	3	2	0	4
	15-16	13	2	5	6	0
	17-19	8	2	2	2	2
	>20	10	2	0	5	3
Kerguelen	8-10	25	5	11	2	7
Syowa	11-12	24	7	2	5	10
	13-14	26	9	8	2	7
	15-16	27	5	11	8	3
	17-19	20	6	3	6	5
	20-23	22	4	4	10	4
	>24	12	3	0	6	3
South Pole	8-12	12	2	2	2	6
Terre Adelie	13-14	10	4	4	1	1

Novolazarev'a	15-16	10	2	4	1	3
	17-19	8	3	1	2	2
	20-23	12	2	4	4	2
	>24	8	2	0	5	1

4.2. Test of log-normal distribution model

Figure 5 shows sample cumulative amplitude-probability distributions representative of a low level of geomagnetic activity (Ap < 12). Examples at two different times of day are shown for Halley equator ward fringe of the auroral zone, for Syowa at the centre of the auroral zone and for Terre Adelie pole ward of the auroral zone. The scales have been chosen so that a log-normal distribution of the absorption expressed in decibels produces a straight line. The dashed line corresponds to a best-fit for all data points and the solid line to data points only within the 0.3-2.0 dB range. The latter fit is more significant because it omits the least accurate absorption values. Values exceeding about 3 dB are much less frequent and thus the distributions for these may be statistically less significant. Rather than quoting regression coefficients for each of the fitted straight lines, a statistics of differences between observed and best-fit values is given below.

The fits of the log-normal model to the data for conditions relevant to high geomagnetic activity level (Ap > 24) are shown in Figure 6. Here Kerguelen is used to represent locations on the equator ward fringe of the auroral zone while South Pole those on the pole ward side. Both of these stations are at lower magnetic latitudes than their counterparts in Figure 5. This selection is thought to be consistent with the known equator ward movement of the zone for periods of increased magnetic activity level.

The fits of the log-normal model to the data for conditions relevant to low and high solar activity level are tested with cumulative-amplitude distributions for a given time-of-day using values for all days within a given year grouped together (not shown).

As found before for Northern Hemisphere data and some limited Southern Hemisphere values, the log-normal fits provide a good match to the data. The slight tendency of the data to bend at the low values of absorption is rather more pronounced for Syowa at all times for both low and high levels of geomagnetic activity. This is most likely related to the particular scaling procedure used (M. Kunitake, private communication). This underestimates the lower and higher values of absorption, say 0.1 to 0.3 dB and above 3 dB. Northern Hemisphere distributions for which could be regarded corresponding conditions (Dixon Island, 73.5N; 80.4E), do not show such marked bending.

The quality of fit of the log-normal distributions can be assessed for Kerguelen and Syowa, for which there exists the longest data sets. The results are shown in Figures 7 and 8 where the data have been combined for all times of day, but sorted out according to levels of geomagnetic activity. Plotted in these figures are the percentage of time, Q_A, that a given absorption, A, is exceeded, as observed and as obtained from the best-fit log-normal distributions. Values of A are selected to evenly sample the distributions up to 2 dB. The straight lines represent equality between observed and best-fit percentages. Table 3 gives the number of occasions (expressed as percentages) when observed Q_A differs from best-fit Q_A by a fixed amount (which is also a percentage), for A equals 0.1; 0.2; 0.5; 1 and 2, for both Kerguelen and Syowa.

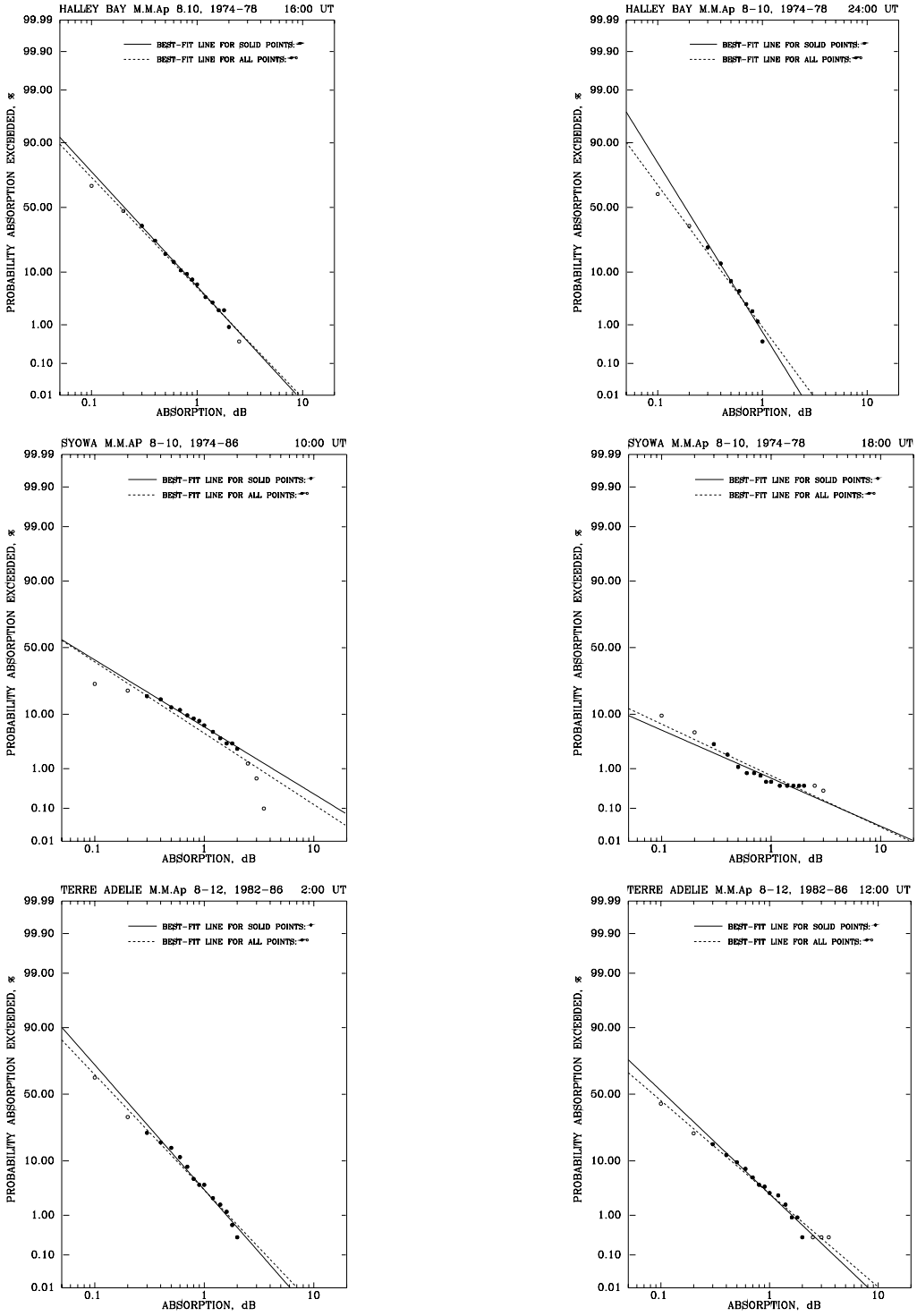

Figure 5. Cumulative amplitude-probability distributions of riometer absorption for Halley Bay (61.0 corrected geomagnetic latitude), Syowa (66.1) and Terre Adelie (80.7), corresponding to conditions of low geomagnetic activity level (Monthly Mean Ap 8-12 for Terre Adelie, 8-10 elsewhere). Lines are for best-fit log-normal distributions.

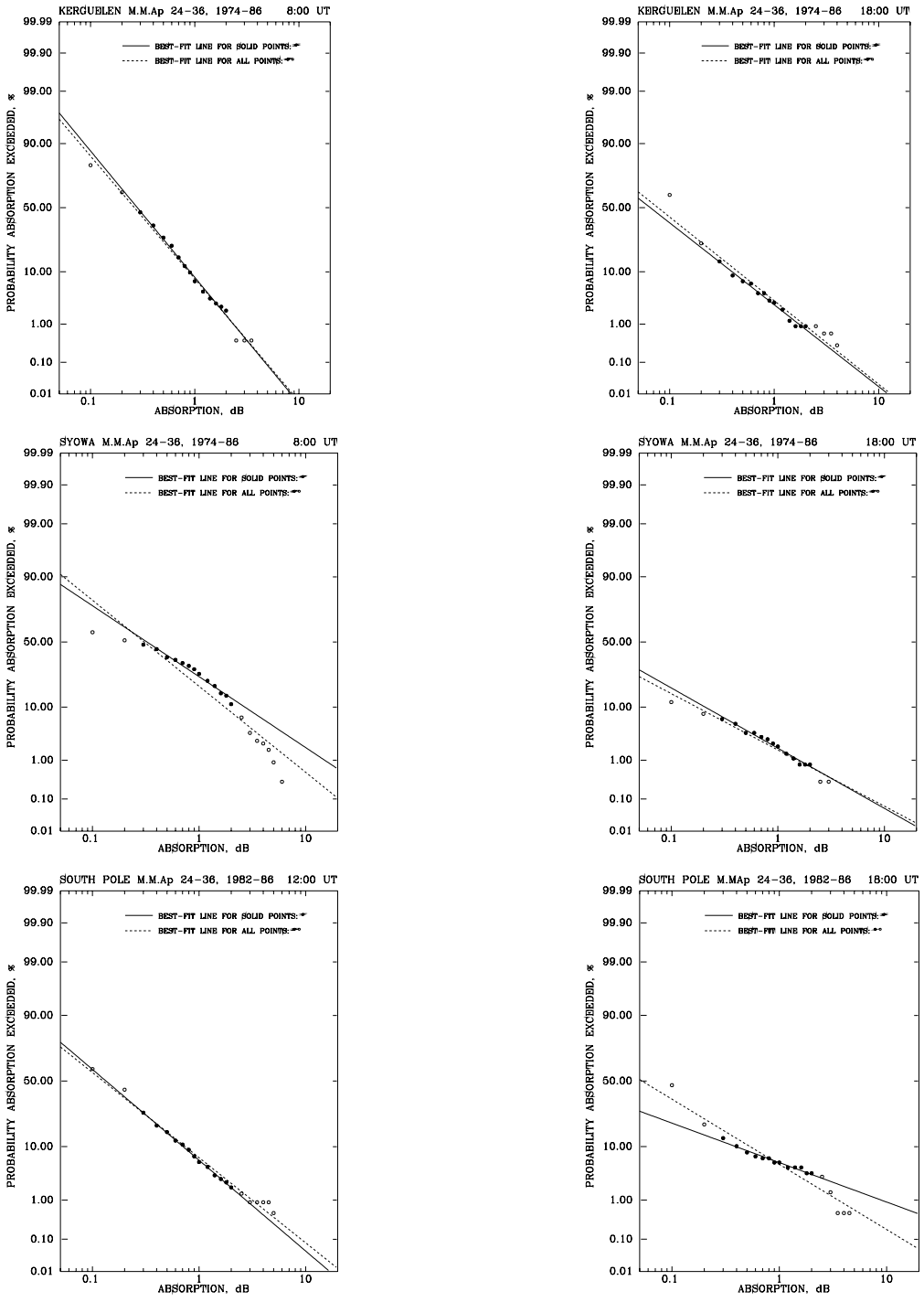

Figure 6. Cumulative amplitude-probability distributions of riometer absorption for Kerguelen (58.4 corrected geomagnetic latitude); Syowa (66.1) and South Pole (74.0), corresponding to conditions of high geomagnetic activity level (Monthly Mean Ap 24-36). Lines are for best-fit log-normal distributions.

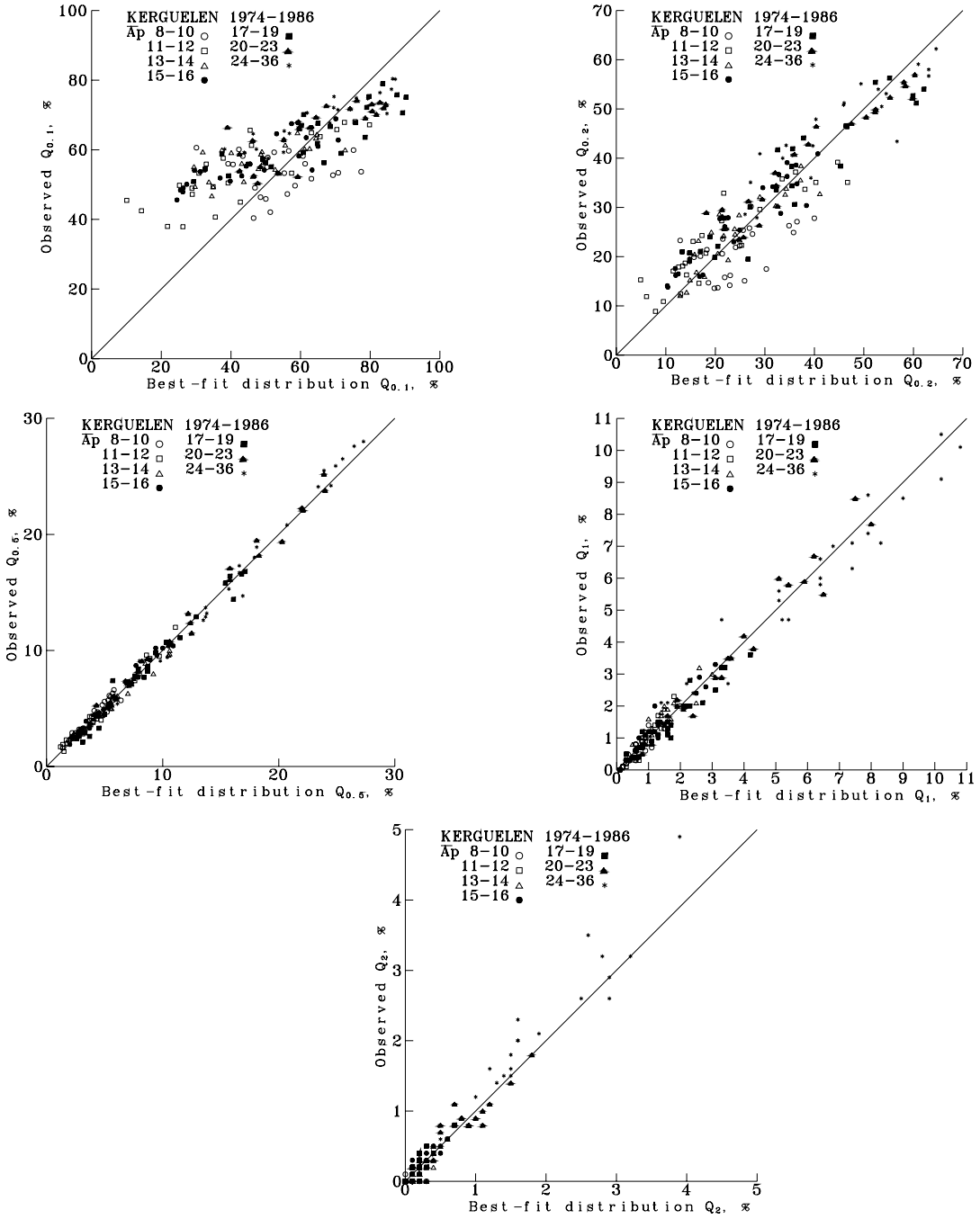

Figure 7. Observed and log-normal best-fit parameters of cumulative amplitude-probability distributions for Kerguelen (58.4 corrected geomagnetic latitude) for a range of geomagnetic activity levels (open circle = monthly mean Ap 8-10; open square = 11-12; open triangle = 13-14; filled circle = 15-16; filled square = 17-19; filled triangle = 20-23; star = 24-36) . Q_A is percentage of time riometer absorption of A dB is exceeded. Lines are for observed equal best-fit parameter.

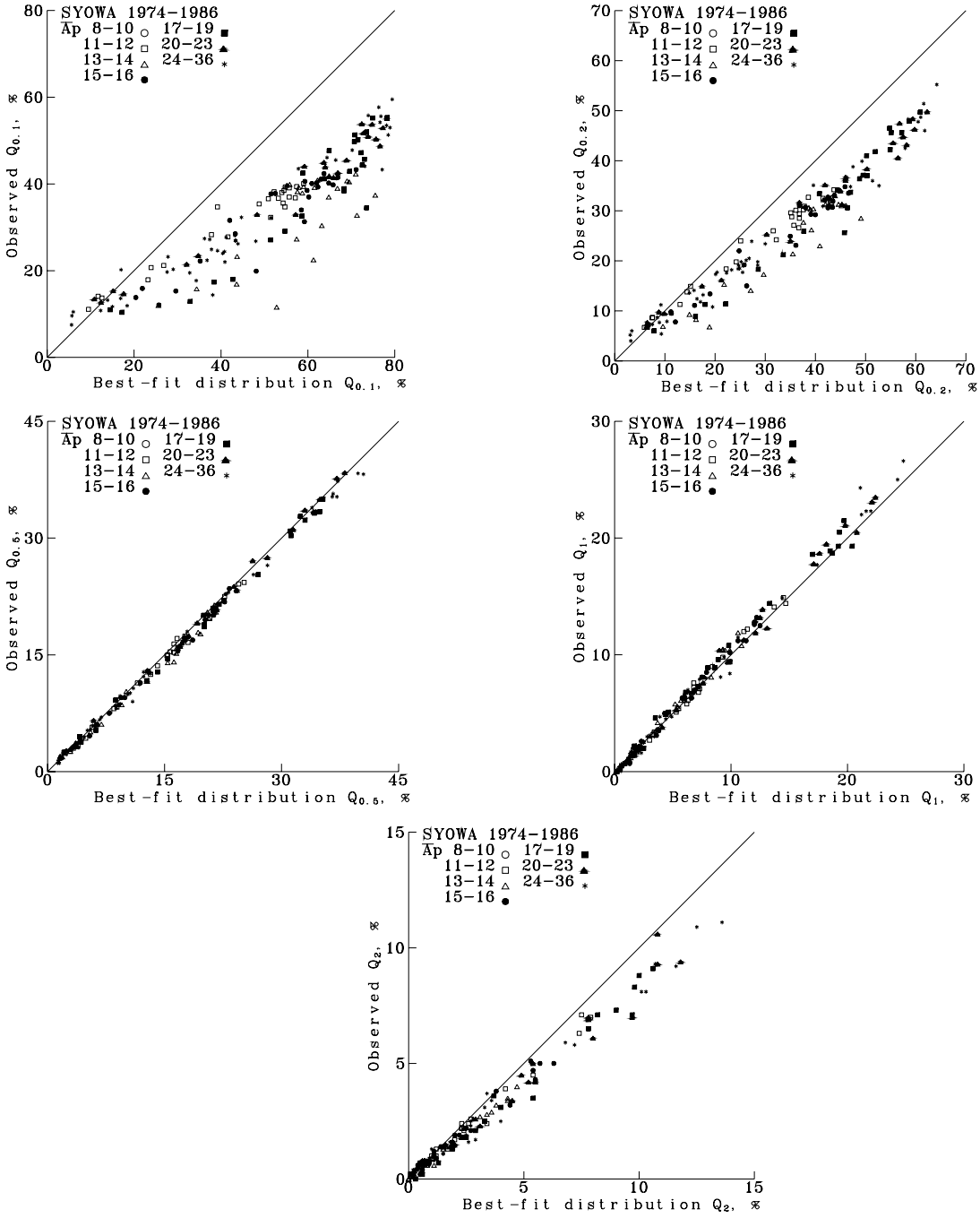

Figure 8. Observed and log-normal best-fit parameters of cumulative amplitude-probability distributions for Syowa (66.1 corrected geomagnetic latitude) for a range of geomagnetic activity levels (open circle = monthly mean Ap 8-10; open square = 11-12; open triangle = 13-14; filled circle = 15-16; filled square = 17-19; filled triangle = 20-23; star = 24-36). Q_A is percentage of time riometer absorption of A dB is exceeded. Lines are for observed equal best-fit parameter.

Kerguelen results confirm that the log-normal model is quite appropriate for values larger than $Q_{0.1}$. There is no obvious dependence either on geomagnetic or solar activity level. These same results are found to apply to all other stations for all sampled conditions, except for Syowa where the log-normal distributions hold only for a more restricted range of Q_A, namely for values greater than 0.2 and less than 2.0 dB.

Table 3. Frequency occurrence (%) of observed distribution Q_A minus best-fit distribution Q_A (Delta Q_A), for given A, which fall within given interval.

	Kerguelen		Syowa	
Difference	Interval	Frequency	Interval	Frequency
Delta $Q_{0.1}$	-10 to 10	73.0	-30 to -10	85.7
Delta $Q_{0.2}$	-5 to 5	83.9	-15 to -5	82.2
Delta $Q_{0.5}$	-0.5 to 0.5	81.6	-1 to 0	81.5
Delta $Q_{1.0}$	-0.5 to 0.5	94.6	-1 to 1	97.1
Delta $Q_{2.0}$	-0.2 to 0.2	93.2	-0.5 to 0.5	74.4

4.3. Relation between log-normal distribution parameters

As already mentioned, the log-normal distribution is completely specified by two independent parameters. Although there may be reasons to choose a specific pair of parameters, it has been found in practice that A_m, the median absorption, and Q_1 are most convenient for a range of propagation prediction applications. Moreover, a relation between these parameters has been shown of value when the simpler use of amplitude probability distributions is required [3,4,13,14,18].

Figure 9 gives A_m and Q_1 from best-fit distributions for all times of day and stations for which data were grouped by magnetic activity levels. Corresponding values for Novolazarevskaya, which were grouped only by year, also fall within the scatter indicated by Figure 9, as do those appropriate to Northern Hemisphere locations already published.

The Syowa results, when plotted separately, indicate that A_m tends to be slightly smaller when compared with that for all other stations for similar geophysical conditions. Recall, however, that the Syowa values include distributions that bend to the low end. Moreover, there is a tendency for A_m values less than about 0.175 to be associated with values of Q_1 close to zero. These should be viewed with caution since they are for the low absorption range of riometer measurements, which are least accurate. Hence, it is here considered reasonable to keep the same approximate relationship between Q_1 and A_m already proposed, namely $A_m = 0.02Q_1$, which is consistent with A_m being 1 dB for Q_1=50%, and zero for Q_1=0, respectively.

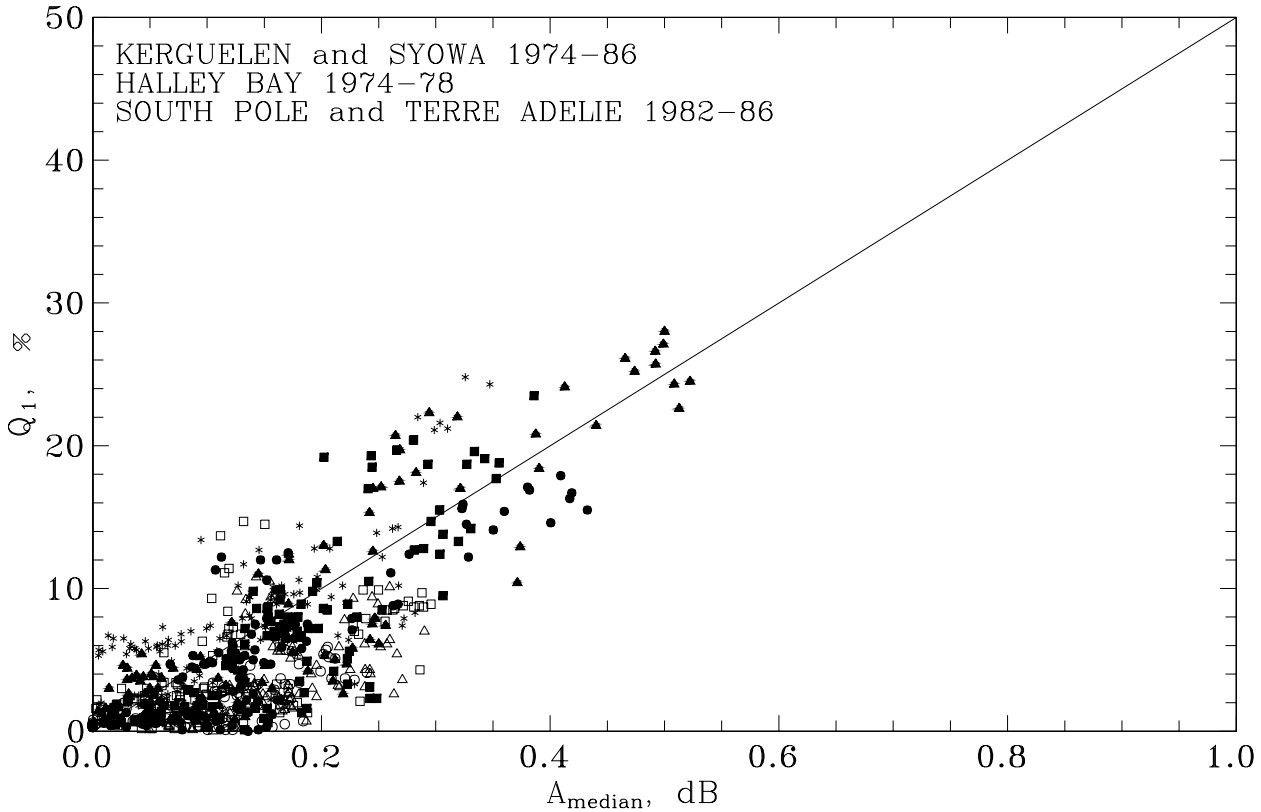

Figure 9. Percentage of time riometer absorption exceeds 1 dB, Q_1, and median absorption, A_m, at a given time of day for Kerguelen (66.1 corrected geomagnetic latitude), Syowa (66.1), Halley Bay (61.0), South Pole (74.0) and Terre Adelie (80.7). Open symbols are for monthly mean Ap < 15, full and star for Ap ≥ 15, respectively. Line is for equation $A_m=0.02Q_1$.

5. TIME-OF-DAY DEPENDENCE

Time-of-day dependencies of parameters of cumulative amplitude-probability distributions were analyzed for all locations and geophysical conditions and found to have common features when grouped according to longitude sectors and proximity to the SAA. Figure 10 corresponds to locations on the equatorial fringe of the auroral zone nearest to the SAA as illustrated for Halley Bay for a range of geomagnetic activity levels. A double daytime maximum and an evening minimum are apparent in all cases. By contrast, diurnal variations for the auroral zone centre and pole ward fringe in the same general longitude sector, a morning and midnight maxima and evening minima are observed as found in most cases for the NH. These are shown in Figures 11 and 12 for Syowa and South Pole, respectively. Note that variations of $Q_{0.5}$ dB instead of Q_1 are plotted for South Pole because auroral absorption is less intense and frequent there. It is also apparent that in this latter case the diurnal variation seems to modulate a kind of background level. This feature, which is common to Terre Adelie, may be related to the incidence of polar cap absorption. Time-of-day variation for Kerguelen, the other equator ward fringe location away from the SAA (Figure 13), is similar to those for Syowa but the timing of the maxima and minima are somewhat displaced.

In Figures 10 to 13 NH model adapted values are also shown. Values are calculated assuming that latitude, time-of-day, season and geomagnetic activity dependencies are the same as the ones that apply for the NH.

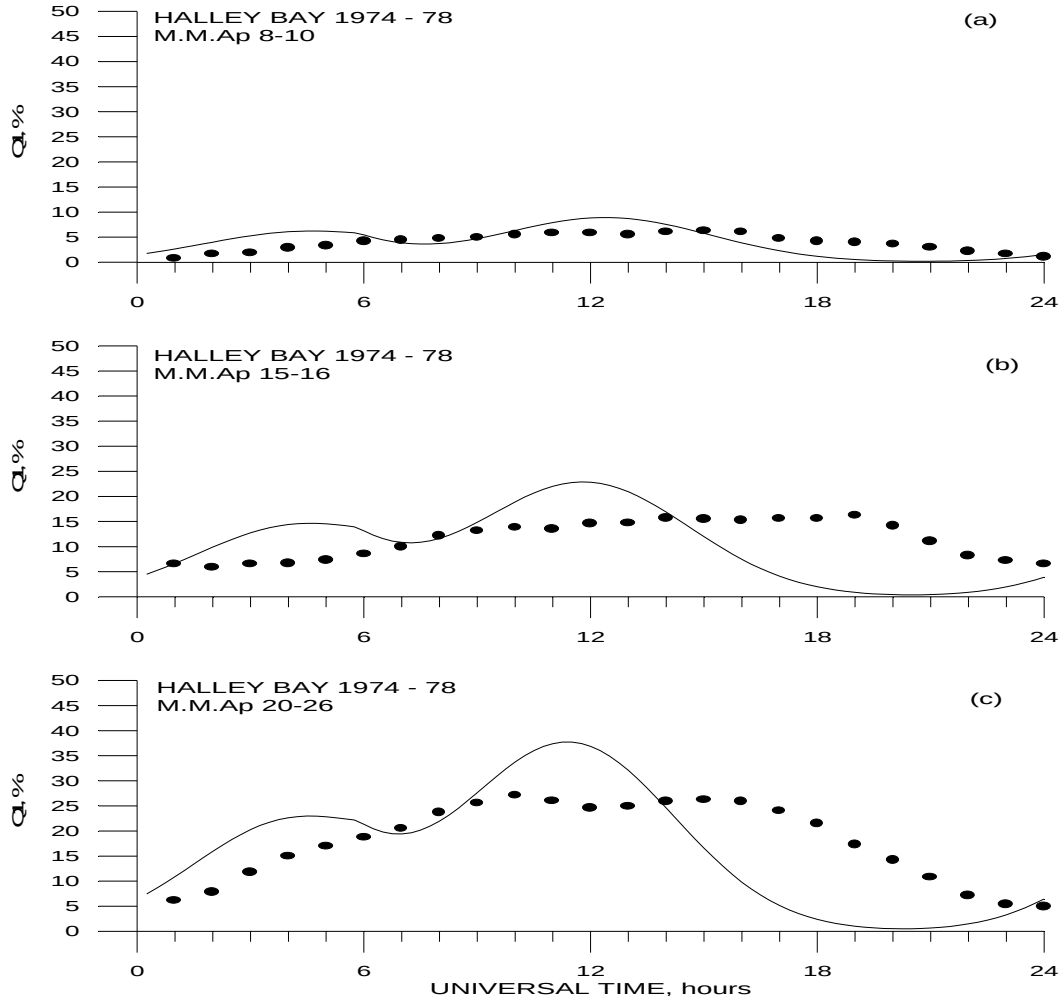

Figure 10. Diurnal variation of percentage of time riometer absorption exceeds 1 dB, Q_1, for Halley Bay (61.0 corrected geomagnetic latitude) corresponding to different levels of geomagnetic activity as measured by monthly mean Ap. (Filled circles) observed hourly values. (full line) NH adapted model. (a) 8-10, (b) 15-16 and (c) 20-26.

Table 4. Corrected geomagnetic longitude factors used to reproduce Southern Hemisphere absorption diurnal variations.

Station	Corrected geomagnetic longitude, degrees	Corrected geomagnetic longitude factor NH	Corrected geomagnetic longitude factor SH	Ratio
Kerguelen	121.4	0.47	1.60	3.4
Halley Bay	28.3	0.16	2.15	13.4
Novolazarev'a	51.5	0.16	1.85	11.6
Syowa	70.9	0.16	0.60	3.8
South Pole	19.5	0.16	0.50	3.1

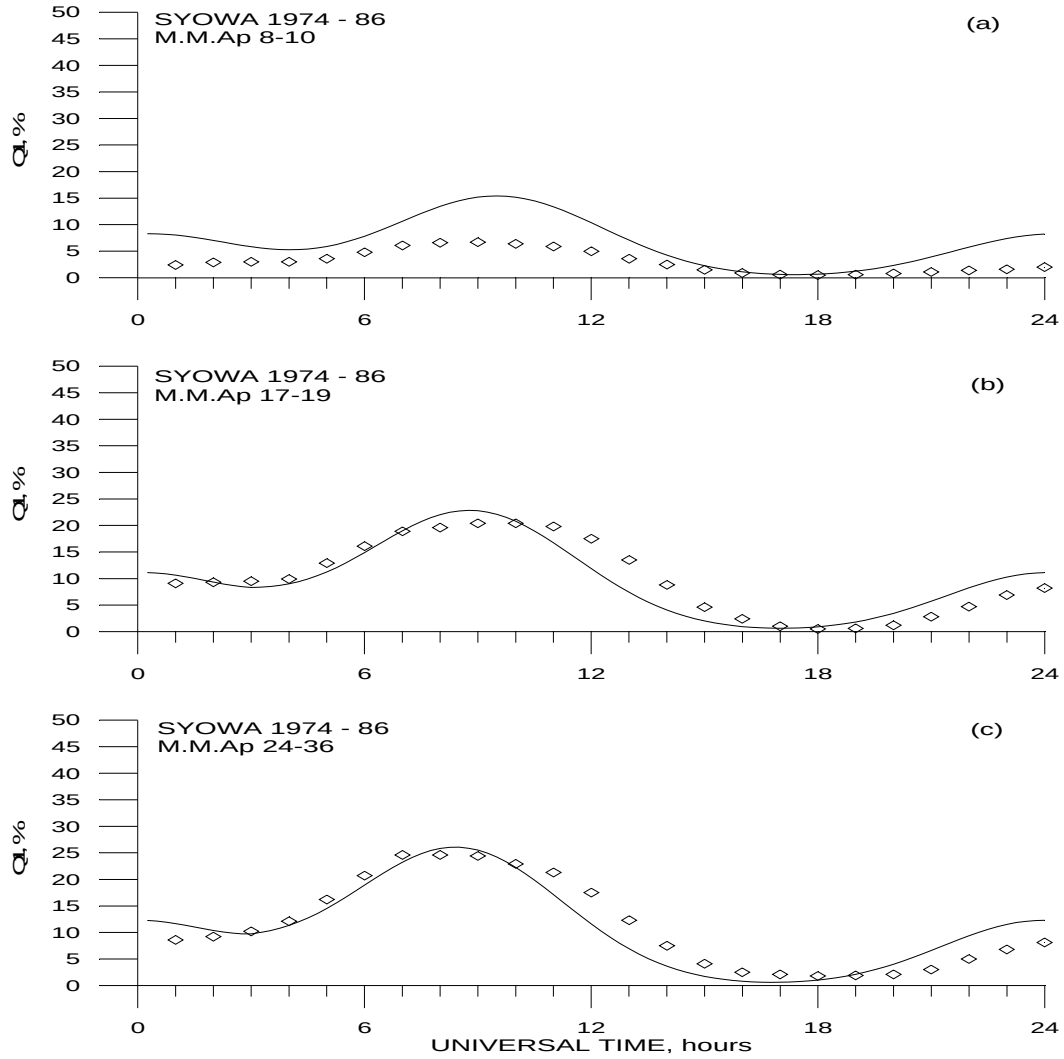

Figure 11. Diurnal variation of percentage of time riometer absorption exceeds 1 dB, Q_1, for Syowa (66.1 corrected geomagnetic latitude) corresponding to different levels of geomagnetic activity as measured by monthly mean Ap. (Filled circles) observed hourly values. (full line) NH adapted model. (a) 8-10, (b) 15-16 and (c) 24-36.

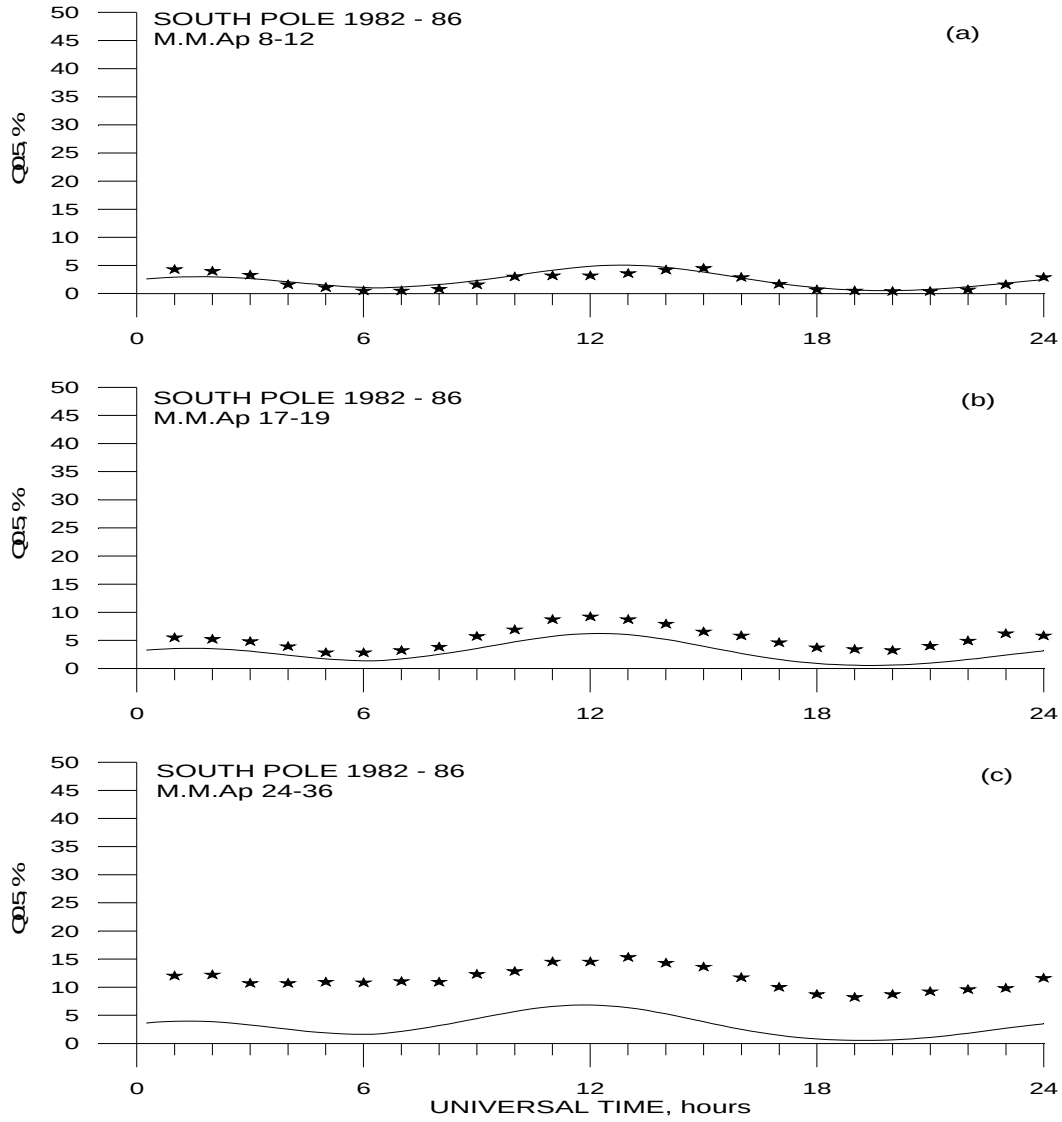

Figure 12. Diurnal variation of percentage of time riometer absorption exceeds 0.5 dB, $Q_{0.5}$, for South Pole (74.0 corrected geomagnetic latitude) corresponding to different levels of geomagnetic activity as measured by monthly mean Ap. (Filled circles) observed hourly values. (full line) NH adapted model. (a) 8-12, (b) 17-19 and (c) 24-36.

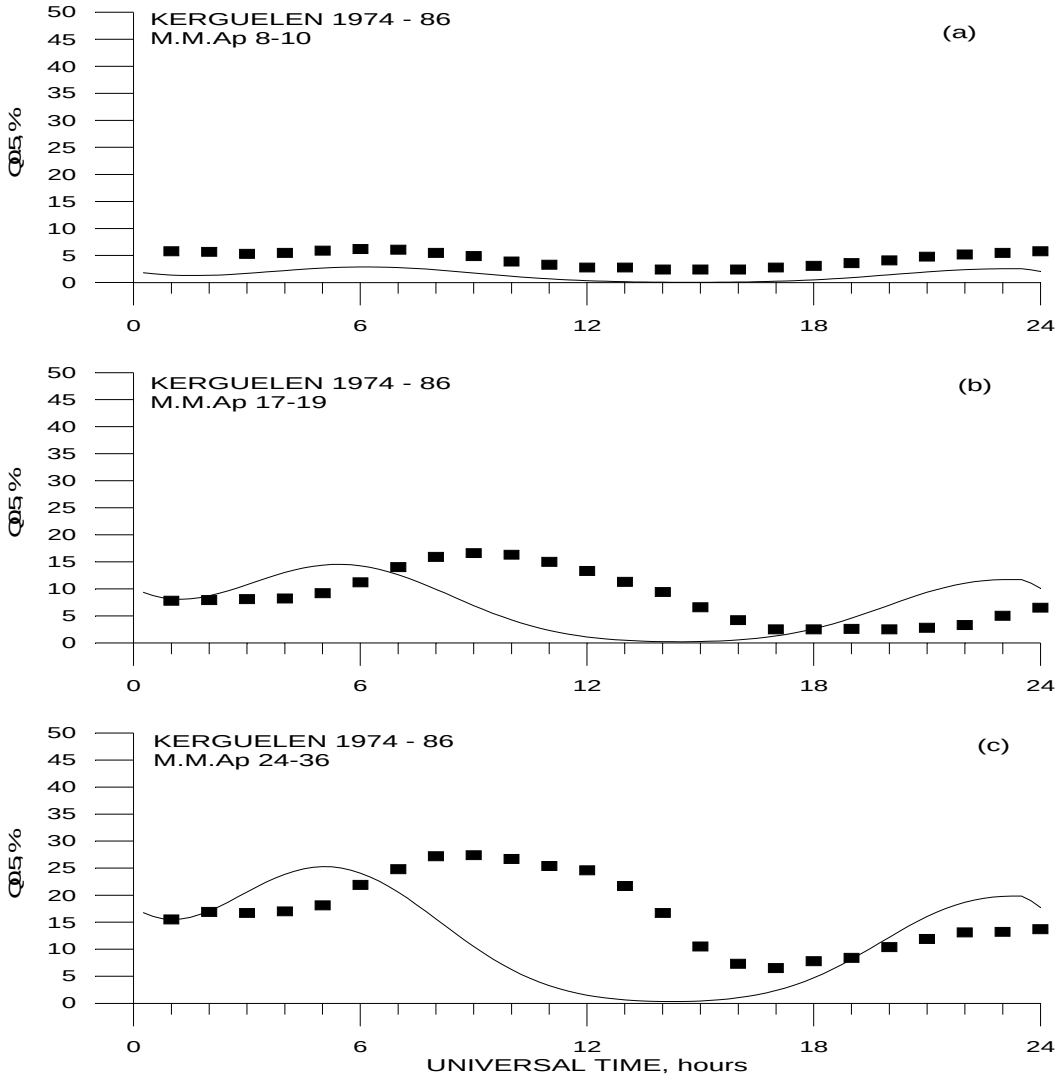

Figure 13. Diurnal variation of percentage of time riometer absorption exceeds 0.5 dB, $Q_{0.5}$, for Kerguelen (58.4 corrected geomagnetic latitude) corresponding to different levels of geomagnetic activity as measured by monthly mean Ap. (Filled circles) observed hourly values. (full line) NH adapted model. (a) 8-12, (b) 17-19 and (c) 24-36.

Only the longitudinal dependence is assumed to be different. Since there is no way to derive this dependence, a simple factor has been determined so as to obtain the best fit of the model values to the observed time-of-day variation of absorption. Table 4 gives these factors for all locations used, except Terre Adelie, which is far from the auroral absorption zone. These factors are discussed in Section 7.

6. LATITUDE DEPENDENCE

Figure 4 clearly shows that there are no locations which could be considered as a latitude chain, i.e. covering a range of latitudes for a given longitude. Thus, determining a latitude dependency of Q_1 requires assembling Q_1 values from different longitudes, which as indicated before cannot be directly compared if there is a longitude dependence. Figure 14 shows NH model Q_1 corresponding to the morning and night maxima, and to the evening minima for a given geomagnetic level. Observed Q_1 values shown have been normalized so as to correspond to a longitude for which the longitude factor is 1, using the longitude factors of Table 4. The comparison of model and observed Q_1 seems to confirm that the SH riometer absorption studied here is latitude dependent following a Gaussian function as it is observed in the NH. This also confirms previous studies that find similar latitude dependence using a restricted data base [e.g.19].

7. LONGITUDE DEPENDENCE

Finally, a kind of longitude dependence of Q_1 could be suggested by extrapolation of the longitude factors already used to determine the time-to-day and latitude dependencies. The longitude factors are compared in Figure 15 with the apparent longitude dependence of particle precipitation determined using some satellite observations [20], and with the longitude dependence found for the NH riometer absorption. These results are also generally consistent with other studies of particle precipitation which do group data according to both magnetic local time and universal time [21, and references within]. It seems that the longitude factors are consistent with the SH satellite observations and suggest that the longitude dependence of riometer absorption in the SH is significantly different from the one that applies for the NH. Although the recent maps of electron precipitation already available [22] include data for all universal time sectors, it may be possible soon to produce maps for different longitude sectors because the original data are indeed binned according to universal time sectors.

8. OTHER DEPENDENCIES

The NH model does include separate Q_1 dependence on geomagnetic activity level giving increased absorption for increasing level, i.e. not included as secondary dependencies on main time-of-day and latitude dependencies. These same separate dependencies are assumed to apply for the SH, and have already been taken into account when comparing observed absorption values with model values for both the time-of-day and latitude dependencies.

The NH model also includes a season dependence. However, as mentioned in Section 4, observed value sample sizes preclude specifying a seasonal dependence for the SH. Thus, again the same season dependence for the NH is considered to apply for the SH.

9. CONCLUSIONS

Measured riometer absorption data for a range of Southern Hemisphere geomagnetic high latitude locations at a given hour are shown to be approximately statistically distributed in accordance with a log-normal distribution model. This result does not seem to depend on time-of-day, latitude, longitude, and solar and geomagnetic activity level for the data sampled. This confirms that results previously found for the NH also apply to the SH riometer absorption.

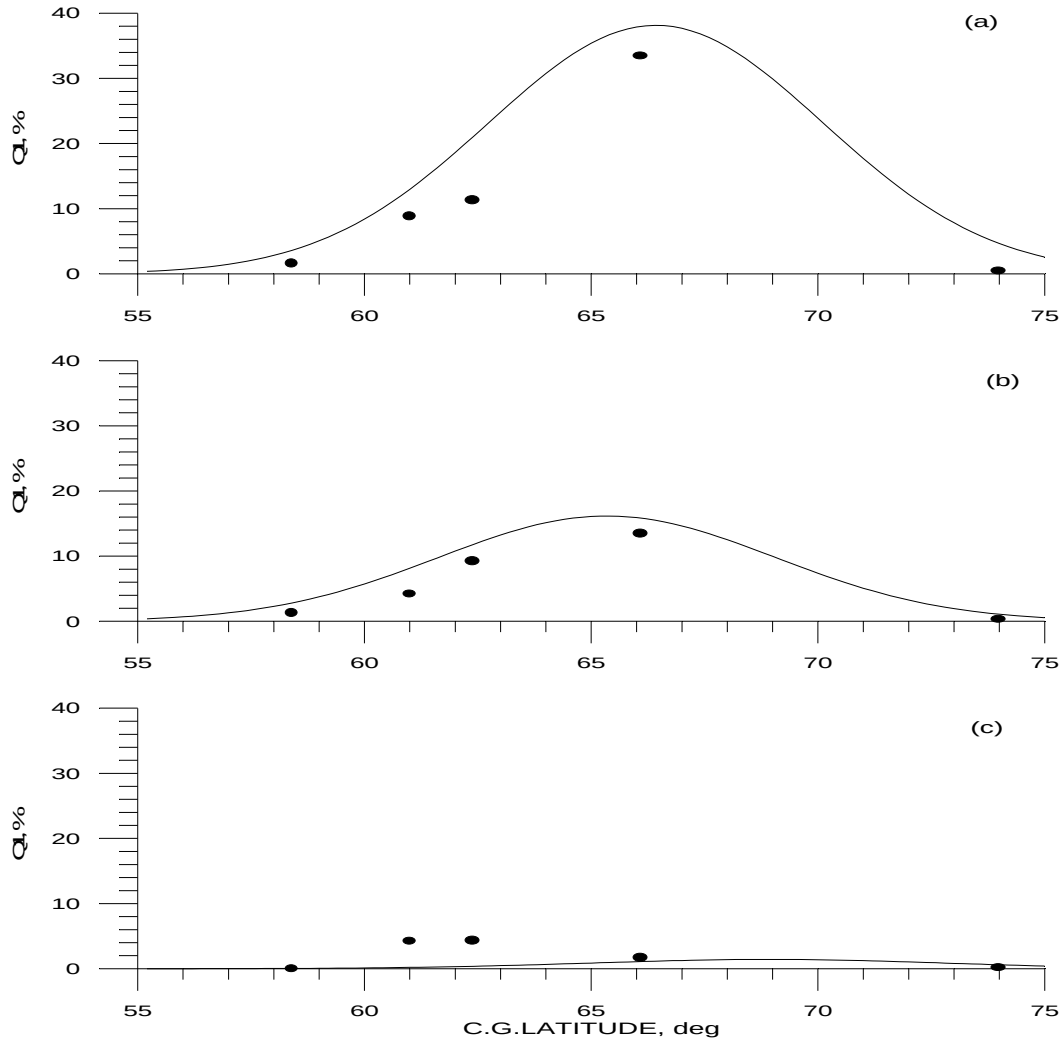

Figure 14. Latitudinal dependence of Q_1, percentage of time absorption at 30 MHz exceeds that of 1 dB, corresponding to a given geomagnetic activity level (Ap=17-19). Values for Equinox (solar declination 0 degrees). (Filled circles) hourly values. (solid line) NH adapted model values. (a) morning maximum, (b) night secondary maximum and (c) evening minimum. Corrected geomagnetic latitude and local time are used.

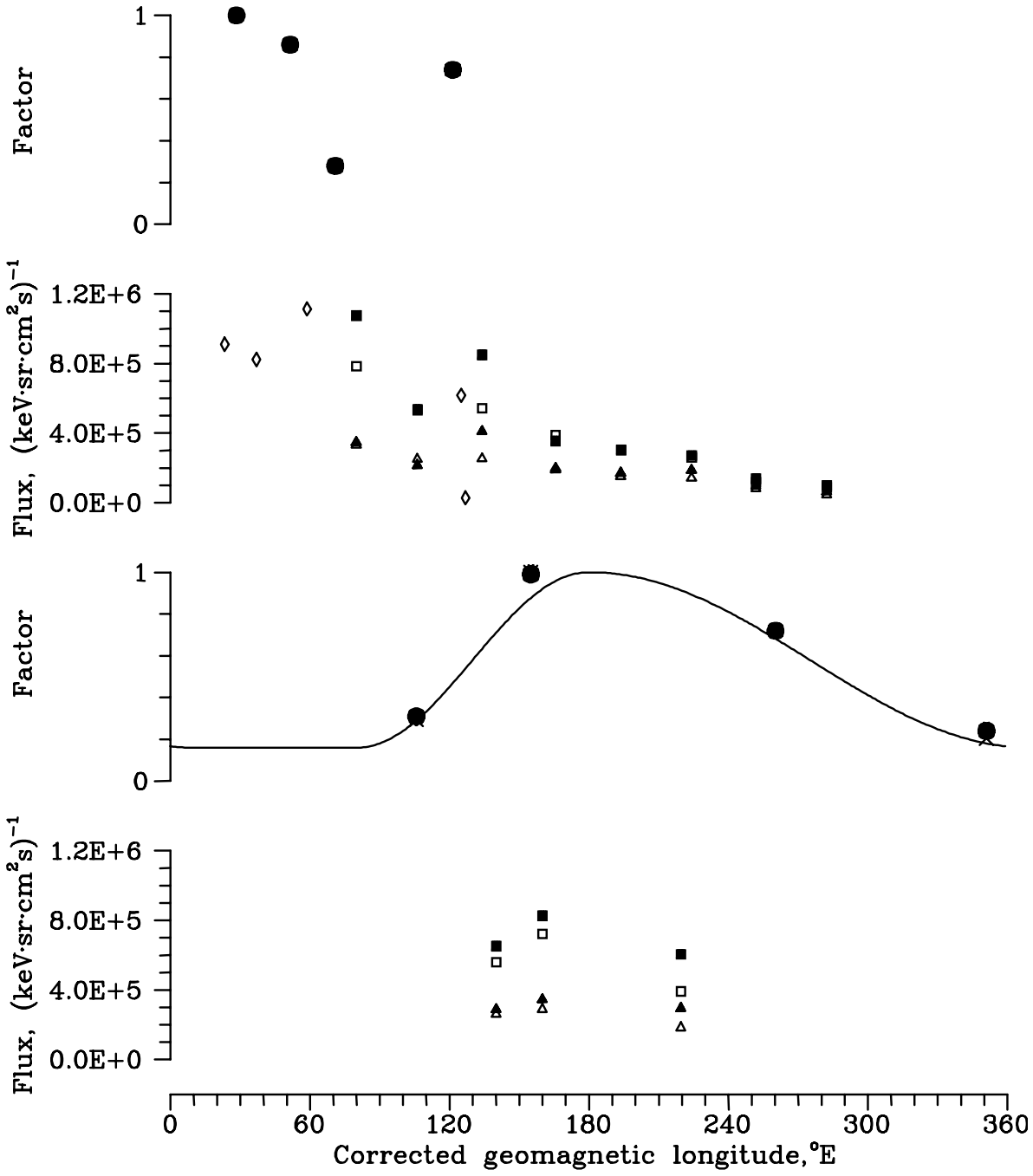

Figure 15. Longitude variation of auroral radio absorption as estimated using riometers and of precipitated electron fluxes as observed by satellites. (a) longitudinal dependence of absorption observed in the Southern Hemisphere. (b) fitted Gaussian latitude distributions flux maxima for longitude sectors in the Southern Hemisphere, magnetic local time 5 to 13 hours, Kp 3 to 6. (open squares and triangles) all flux values considered and (filled squares and triangles) only median flux values for 2° latitude intervals considered, for Meteor, 10 and 20 keV, respectively. (oblongs) Intercosmos-Bulgaria 1300, 10.8 keV. (c) longitudinal dependence of absorption observed in the Northern Hemisphere [Foppiano and Bradley, 1983] (d) same to (b) for Meteor, Northern Hemisphere.

The time-of-day dependences of parameters of log-normal distributions found for locations in the SH are similar to the ones for the NH only for locations away from the so-called South Atlantic Anomaly of the geomagnetic field.

The latitudinal dependence also seems to be similar to that in the NH, although further confirmation should be pursued due to the restricted spatial coverage of the data used.

The longitudinal dependence seems to be different from that in the NH, probably been consistent with that found for satellite particle precipitation data which has been grouped according to both local and universal time.

Auroral riometer absorption seems to be much larger in the South Atlantic Anomaly longitude sector than in the geomagnetic conjugate sector in the NH.

ACKNOWLEDGEMENTS

Riometer data were kindly made available by Madame D. Fouassier (Kerguelen and Terre Adelie), J.R. Dudeney (Halley Bay), H. Gernandt (Novolazarevskaya) and T.J. Rosenberg (South Pole).

The development of the data base and preliminary analyses were supported by NSF grants INT-8815373 and DPP-9119753 to T.J. Rosenberg while I was on sabbatical leave at the University of Maryland, U.S.A., from Universidad de Concepción when the work was started. Almost all the rest of the work was supported by the National Institute of Polar Research, Japan, which funded my research stay there. Support for this study has also come from the Chilean Fondo Nacional de Desarrollo Científico y Tecnológico under Proyecto N^{o} 1940934.

Annex

The percentage probability, Q_A, that an absorption A dB is exceed, is given as:

$$Q_A = \frac{100}{\sqrt{2\pi}} \int_{\frac{\log_e A - \log_e A_m}{\sigma}}^{\infty} \exp\left[-\frac{y^2}{2}\right] dy$$

Where A_m is the median absorption. Thus, both Q_A for a given A and A_m are required to determine σ so as to specify the log-normal distribution. As indicated before, choosing Q_1 and A_m are particularly convenient. The model gives A_m from Q_1 as

$A_m = 0.02 Q_1$ and Q_1 as the sum of two terms (drizzle and splash precipitation associated terms)

$Q_1 = Q_{1d} + Q_{1s}$ with $Q_{1d} = 21 d_\lambda d_T d_R d_\theta d_M$ and $Q_{1s} = 12 s_\lambda s_T s_R s_\theta s_M$,

where λ, T, R, θ and M are main dependencies on latitude, time-of-day, solar activity or geomagnetic activity (*), and month.

$$d_\lambda = \exp\left[\frac{-(\lambda-\lambda_m)^2}{2\sigma^2}\right], \text{ where } \lambda_m = 68(1-0.0004R) \text{ and } \sigma_\lambda = 3(1+0.004R),$$

$$d_T = \exp\left[\frac{-(t_1-T_m)^2}{15.7}\right], \text{ with } T_m = 10(1-0.002R) \text{ and } t_1 = T \text{ for } 0 \le T \le T_m + 12 \text{ or}$$

$$t_1 = T - 24 \text{ for } T_m + 12 < T < 24$$

$$d_R = 1 + 0.014R$$

$d_\theta = 0.58 - 0.42 \sin [0.947(\theta + 85^o)]$ for $0 \le \theta < 10$

$= 0.16$ for $10 \le \theta < 80$

$= 0.58 + 0.42 \sin [1.80\ \theta - 130^o)]$ for $80 \le \theta < 180$

$= 0.58 - 0.42 \sin [0.947\ (\theta - 275^o)]$ for $180 \le \theta < 360$

$$d_M = 1 - 0.3 \sin 3.86\delta$$

$$s_\lambda = \exp\left[\frac{-(\lambda-\lambda_m{}^1)^2}{2\sigma_\lambda{}^2}\right], \text{ where } \lambda_m{}^1 = 67(1-0.0006R) + 0.3(1+0.012R)|t| \text{ and}$$

$$t = T - 3 \text{ for } 0 \le T \le 15 \text{ or}$$
$$t = T - 27 \text{ for } 15 < T < 24$$

$$s_T = \exp\left[\frac{-t_2{}^2}{15.7}\right], \text{ where } t_2 = T \text{ for } 0 \le T \le 12 \text{ or } t_2 = T - 24 \text{ for } 12 < T < 24$$

$$s_R = 1 + 0.009R$$

$$s_\theta = d_\theta$$

$$s_M = 1$$

(*) Two empirical relations are used: $R = 33.1\ Kp - 51.6$ (see rationale in Foppiano and Bradley, 1983) and $Kp = (\log(Ap) - 0.3222)/0.2817$ (for easier fitting to SH observed riometer absorption).

REFERENCES

[1] Agy, V. (1972) “A model for the study and prediction of auroral effects on HF radar”, *Radio propagation in the Arctic*, Chapter 32-1. NATO Advisory Group for Aerospace Research and Development Conference Proceedings AGARD-CP-97, Neuilly-sur-Seine (France)

[2] Elkins, T.J. (1972) “A model of auroral-substorm absorption”, Air Force Cambridge Research Laboratories Report AFCRL-TR-0413, USAF, L.G. Hanscom Field, Bedford, Massachusetts.

[3] Vondrak, R.R.; Smith, G.; Hatfield, V.E.; Tsunoda, R.T.; Frank, V.R. and Perreault, P.D. (1978) “Chatanika model of the high-latitude ionosphere for application to HF propagation prediction”, Rome Air Development Center Technical Report RADC-TR-78-7, Hanscom Air Force base, Massachusetts.

[4] Foppiano, A.J. and Bradley, P.A. (1983) "Prediction of auroral absorption of high-frequency waves at oblique incidence", Telecommunication Journal (Geneva), 50, 547-560.

[5] Zhulina, E.M., Izraitel, A.G., and Kishcha, P.B. (1990) "An analytic model of auroral absorption with different magnetic disturbances", Geomagnetism and Aeronomy, 30, 441-442

[6] Lucas, D.L. and Haydon, G.W. (1966) "Predicting statistical performance indices for high frequency ionospheric telecommunication systems", Environmental Science Services Administration Technical Report IER-1-ITSA 1, U.S. Government Printing Office.

[7] Bilitza, D. (1992) “Solar-terrestrial model and application software”, Planetary and Space Sciences, 40, 541-579.

[8] Milan, S.E.; Jones, T.B.; Lester, M.; Warrington, E.M. and Reeves, G.D. (1996) “Substorm correlated absorption on a 3200 km trans-auroral HF propagation path”, Annales Geophysicae, 14, 182-190.

[9] Greenberg, E.M. and LaBelle, J. (2002) “Measurement and modeling of auroral absorption of HF radio waves using a single receiver”, Radio Science, 37, pp. 6-1.

[10] Krishnaswamy, S.; Detrick, D.L. and Rosenberg, T.J. (1985) "The inflection point method of determining riometer quiet day curves", Radio Science, 20, 123-136.

[11] Ose, M.and Kurihara, N. (1983) "Riometer records of 30MHz cosmic noise at Syowa Station, Antarctica in 1981", JARE data reports No. 80 (Ionosphere 27), National Institute of Polar Research, Tokyo, Japan.

[12] Rosenberg,T.J.; Detrick, D.L.; Venkatesan, D. and van Bavel, G. (1991) "A comparative study of imaging and broad-beam riometer measurements: The effect of spatial structure on the frequency dependence of auroral absorption, J. Geophys. Res., 96, 17,793-17,803.

[13] Foppiano. A.J. (1975) "A new method for predicting the auroral absorption of HF sky waves, CCIR Interim Working Party 6/1, Documents 3 and 10, International Telecommunication Union, Geneva.

[14] Masi, J.L. (1980) "Radar studies from Point Barrow, Alaska", Ph.D. Thesis, University of London, U.K.

[15] Krishnaswamy, S. (1987) "Statistics of auroral radio absorption at Siple and South Pole", Mem. Natl Inst. Polar Res., Spec. Issue, 48, 287-297.

[16] Foppiano A.J. and Bradley, P.A. (1984) "Day-to-day variability of riometer absorption", Journal of Atmospheric and Terrestrial Physics, 46, 689-696.

[17] Hargreaves, J.K.; Feeney, M.T.; Ranta, H. and Ranta, A. (1987) "On the prediction of auroral radio absorption on the equatorial side of the absorption zone", Journal of Atmospheric and Terrestrial Physics, 49, 259-272.

[18] Hargreaves, J.K. (1966) “On the variation of aurora radio absorption with geomagnetic activity”, Planetary and Space Science, 14, 991-1006.

[19] Hargreaves, J.K. and Cowley, F.C. (1967) “Studies of radio absorption events at three magnetic latitudes- II, differences between conjugate regions”, Planetary and Space Science, 15, 1585-1597.

[20] Stepanova, M.V.; Foppiano, A.J.; Teltzov, M.V. and Feygin V.M. (2000) “Comparative studies of satellite electron flux measurements and riometer auroral absorption estimates in the southern hemisphere (unpublished).

[21] Roble, S.; Sheldon, W.R.; Benbrook, J.R.; Bering, E.A. and Vampola, A.L. (1994) “Investigation of S3-2 satellite data for local time variation of energetic electron precipitation”, Journal of Geophysical Research, 99 (A3), 3845-3854.

[22] Wüest, M.; Frahm, R.A.; Jennings, J.K. and Sharber, J.R. (2005) “Forescasting electron precipitation based on predicted geomagnetic activity”, Advances of Space Research, 36 (12), 2445-2450.

[23] Chisham, G.; Coleman, I.J.; Freeman, M.P.; Pinnock, M. and Lester, M. (2002) “Ionospheric signatures of split reconnection X-lines during conditions of IMF $B_z < 0$ and $|B_y| \sim |B_z|$: Evidence for the antiparallel merging hypothesis”, Journal of Geophysical Research, 107 (A10), 1323, doi:10.1029/2001JA009124, 2002.